



PERGAMON

Building and Environment 34 (1999) 671-679

**BUILDING AND
ENVIRONMENT**

Evaluation of the indoor temperature field using a given air velocity distribution

C.M. Ghiaus, A.G. Ghiaus*

Technical University of Civil Engineering—Bucharest, Building Services Engineering Faculty, Bd. P. Ponişcoiu, 66, RO-73 232 Bucuresti-39, Romania

Received 8 October 1997; received in revised form 6 April 1998; accepted 14 September 1998

Abstract

A new method for compensating the space discretization error introduced when the fixed flow field is considered for the dynamic models of temperature distribution is presented. It is proved that the method generally used in literature is a particular solution of the proposed one. Moreover, it results in a continuous-time model, for which the integrating method becomes a free choice and a state-space representation is possible. The numerical model was experimentally validated, the comparison, both in the time and in the frequency domains, between simulation and measured results showing good agreement. The presented dynamic model increases the calculation speed and it can be analysed with the tools developed in control theory. © 1999 Elsevier Science Ltd. All rights reserved.

Keywords: Dynamic models; Computational fluid dynamic; Air conditioning; Control theory

Nomenclature

S_{ϕ} source term in general transport equation
 S_q source term in thermal energy equation
 V velocity vector
 u, v, w velocity components in x -, y - and z -directions, respectively
 x, y, z space co-ordinates

Greek symbols

Γ effective thermal diffusivity coefficient
 Γ_{ϕ} effective diffusivity coefficient
 θ temperature
 ρ density
 Φ potential in the general transport equation

Subscripts

e, w, n, s, h, l east, west, north, south, high, and low frontier, respectively, for an elementary cell
 E, W, N, S, H, L east, west, north, south, high and low elementary cell, respectively
 i, j, k the current indexes for x -, y - and z -directions, respectively

1. Introduction

In order to evaluate the indoor thermal comfort, it is desirable to know the air flow field and the room temperature distribution [1]. As an alternative to experiment, the computational fluid dynamic (CFD) theory supplies numerical techniques for studying indoor temperature distribution and air flow field (and consequently the thermal comfort) in a computational grid [2-4]. However, since the mass, energy and especially momentum balance equations need thousands of grid cells to be solved by iteration procedure, and since the iterative process should be continued until all dependent variables converge to some satisfactory extent, the CFD calculation takes so much time that it is practically suitable only for some steady state evaluations. Although the future development of computer technology will eventually make fast dynamic CFD calculation possible, at present we have to find some trade-off methods concerning the calculation of the dynamic temperature distributions which is essential for the simulation of indoor climate control systems.

For the problem of indoor air flow, Peng et al. [5] proposed a method to calculate the dynamic temperature distribution in a fixed flow field, provided that it is correctly calculated for the steady state. By assuming that the air flow field is not changing in time and can be correctly calculated by the CFD code, only the dynamic

* Corresponding author: University of Patras, School of Engineering, Fluid Mechanics Laboratory, GR-265 00, Patras, Greece. Tel.: 0030-61-99 7193; fax: 0030-61-99 7202; e-mail: ghiaus@mech.upatras.gr

energy balance equation needs to be solved. But Peng et al. [5] used the implicit (backward difference) method to solve the energy balance equation, thereby the iteration method for all grid cells has to be used. However, the given flow field may not satisfy the continuity equation, a problem which appears in the discretized continuity equation, also mentioned by Patankar [2], who stated that the rule of sum of neighbour coefficients should be satisfied. To correct the discretization error, Patankar [2] considers that the new values (at time $t + \Delta t$) prevail during the time step. The old value (i.e. the one at time t) appears only through its time derivative. The new values are initially guessed. Then, an iterative procedure is applied in order to obtain the values at the instant ($t + \Delta t$). But the iterative procedure is very time consuming. This paper discusses a new method to correct the discretization error, i.e. the mass compensation idea. A mass flow is considered in a supplementary (fictitious) direction so that the continuity equation for each control volume (or cell) and the ones for the overall system are satisfied. This idea will be used in solving the dynamic energy equation when the explicit (forward finite difference) method is used.

2. Mathematical modelling

2.1. Correct of mass balance equation

The prediction of air flow in ventilated rooms is based on the solution of the general transport equation:

$$\frac{\partial}{\partial t}(\rho\Phi) + \text{div}(\rho\mathbf{V}\Phi) = \text{div}[\Gamma_{\Phi}\text{grad}(\Phi)] + S_{\Phi} \quad (1)$$

where Φ , Γ_{Φ} and S_{Φ} (for the k - ϵ model) are given in Table 1 [4].

According to Peng et al. [5], the dynamic model of temperature distribution is mathematically expressed by the thermal energy balance:

$$\frac{\partial}{\partial t}(\rho\theta) + \text{div}(\rho\mathbf{V}\theta) = \text{div}(\Gamma\text{grad}(\theta)) + S_{\theta} \quad (2)$$

with the following assumptions:
constant density:

$$\frac{\partial}{\partial t}\rho = 0; \quad \frac{\partial}{\partial x}\rho = 0; \quad \frac{\partial}{\partial y}\rho = 0; \quad \frac{\partial}{\partial z}\rho = 0; \quad (3)$$

static velocity field:

$$\frac{\partial}{\partial t}\mathbf{V} = 0 \quad (4)$$

2.2. Continuity equation in steady-state for continuous- and discrete-space systems

Computational fluid dynamics (CFD) computer programs solve numerically the set of transport eqns (1), evaluating the flow field. The problem is that the computed velocity field does not satisfy the continuity equation.

A steady-state solution in a discrete space is usually given by CFD programs. The dependent variables Φ (see Table 1) are evaluated at the grid nodes (a typical grid is shown in Fig. 1). This discretization method is known as 'finite volume' method. The grid node convention, presented in Fig. 2, is used to derive the equivalent discretization of eqn (2). The grey area represents the 'control volume' which, for a three-dimensional space, has the faces denoted by e, w, h, l, n and s for east, west, high, low, north and south faces, respectively. For a two-

Table 1
Dependent variables, effective diffusion coefficients and source terms in the general transport equation [4]

Equation	Φ	Γ_{Φ}	S_{Φ}
Continuity	1	0	•
u Momentum	u	μ_e	$-\frac{\partial p}{\partial x} + \frac{\partial}{\partial x}\left(\mu_e \frac{\partial u}{\partial x}\right) + \frac{\partial}{\partial y}\left(\mu_e \frac{\partial v}{\partial x}\right) + \frac{\partial}{\partial z}\left(\mu_e \frac{\partial w}{\partial x}\right)$
v Momentum	v	μ_e	$-\frac{\partial p}{\partial y} + \frac{\partial}{\partial x}\left(\mu_e \frac{\partial u}{\partial y}\right) + \frac{\partial}{\partial y}\left(\mu_e \frac{\partial v}{\partial y}\right) + \frac{\partial}{\partial z}\left(\mu_e \frac{\partial w}{\partial y}\right) - g(\rho - \rho_0)$
w Momentum	w	μ_e	$-\frac{\partial p}{\partial z} + \frac{\partial}{\partial x}\left(\mu_e \frac{\partial u}{\partial z}\right) + \frac{\partial}{\partial y}\left(\mu_e \frac{\partial v}{\partial z}\right) + \frac{\partial}{\partial z}\left(\mu_e \frac{\partial w}{\partial z}\right)$
Temperature	θ	Γ_c	q/C_p
Kinetic energy	k	Γ_k	$G_s - \rho\epsilon + G_B$
Dissipation rate	ϵ	Γ_ϵ	$C_1 \frac{\epsilon}{k}(G_s + G_B) - C_2 \rho \frac{\epsilon^2}{k}$

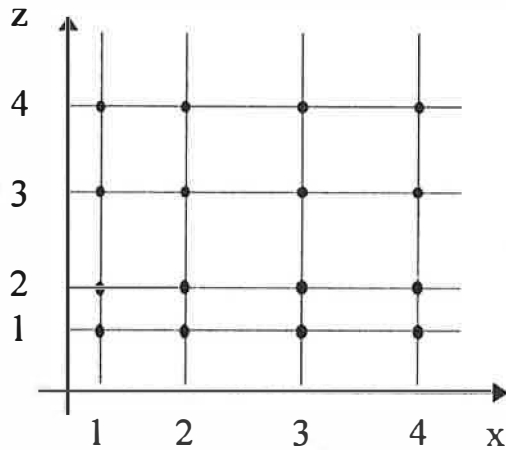


Fig. 1. Grid generation for the two-dimensional numerical simulation.

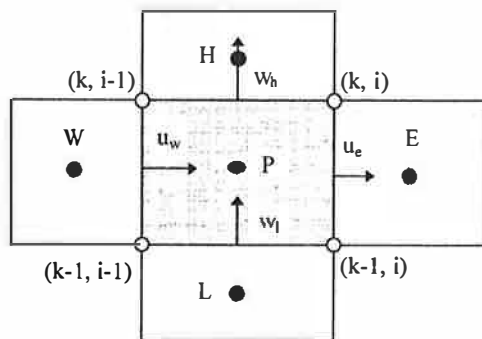


Fig. 2. The control volume for a two-dimensional cell.

dimensional space, the faces are denoted by e, w, h, and l. Integrating eqn (2) over the control volume, it becomes:

$$\begin{aligned} \frac{\partial}{\partial t}(\rho\theta) = & -\frac{(\rho u\theta)_e - (\rho u\theta)_w}{\Delta x} \\ & -\frac{(\rho v\theta)_n - (\rho v\theta)_s}{\Delta y} - \frac{(\rho w\theta)_h - (\rho w\theta)_l}{\Delta z} \\ & + \frac{\left(\Gamma \frac{\partial\theta}{\partial x}\right)_e - \left(\Gamma \frac{\partial\theta}{\partial x}\right)_w}{\Delta x} + \frac{\left(\Gamma \frac{\partial\theta}{\partial y}\right)_n - \left(\Gamma \frac{\partial\theta}{\partial y}\right)_s}{\Delta y} \\ & + \frac{\left(\Gamma \frac{\partial\theta}{\partial z}\right)_h - \left(\Gamma \frac{\partial\theta}{\partial z}\right)_l}{\Delta z} + S_\theta \end{aligned} \quad (5)$$

Let us call 'discrete divergence' the form derived by integrating the differential equation over the control volume shown in Fig. 2. Then, the discrete divergence of the velocity field, as calculated by CFD codes for steady-state conditions, may be not identically null when the continuous divergence of the velocity field is null. This may be due to:

- Insufficient convergence achieved by the applied iter-

ative procedure. More iterations will decrease the value of discrete divergence.

- Error introduced by discretization. Since the velocity is a non-linear function with respect to space co-ordinate, the difference between the divergence and its numerical approximation is present in the most of the cases.

We will prove that the discrete divergence may be not identically null, when the continuous divergence is null, i.e. $\exists(i, j, k)$ so that:

$$\text{div d}(\mathbf{V}_{ijk}) \equiv \frac{u_e - u_w}{\Delta x} + \frac{v_n - v_s}{\Delta y} + \frac{w_h - w_l}{\Delta z} \neq 0 \quad (6)$$

when $\text{div}(\mathbf{V}) = 0$.

If the velocity function is not linear, then it is possible for the derivative in point P' and the finite difference in point P to be different (see Fig. 3):

$$\frac{\partial}{\partial x} u \neq \frac{u_e - u_w}{\Delta x}; \quad \frac{\partial}{\partial y} v \neq \frac{v_n - v_s}{\Delta y}; \quad \frac{\partial}{\partial z} w \neq \frac{w_h - w_l}{\Delta z}; \quad (7)$$

and consequently the divergence may differ its discrete form.

But, when continuous-time discrete-space steady flow models are considered, the conservation of mass must be satisfied for each elementary cell volume, that is:

$$\forall(i, j, k) \text{div d}(\mathbf{V}_{ijk}) = 0 \quad (8)$$

2.3. Correction of discrete continuity equation

The space discretization introduces an error in the mass balance equation. This error should be corrected so that the continuity equation is also satisfied in discrete space [6].

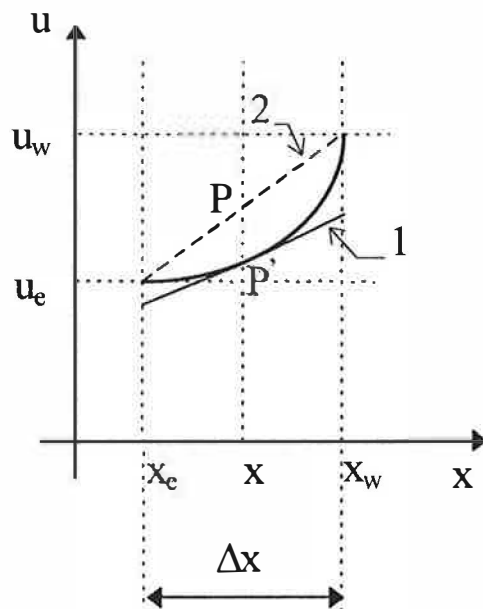


Fig. 3. The derivative (1) and the finite difference (2) for a non-linear velocity function.

The continuity equation in discrete form, for a three-dimensional space, without internal mass sources:

$$\rho \Delta y \Delta z (u_e - u_w) + \rho \Delta x \Delta z (v_n - v_s) + \rho \Delta x \Delta y (w_h - w_l) = 0 \tag{9}$$

will be considered as the continuity equation (or mass balance equation) for the discrete-space. To simplify the presentation, let us assume a two-dimensional space (x, z), which is the vertical plane. In this space, the unbalanced mass of a cell is compensated in order to have the continuity equation satisfied for a continuous-time discrete-space steady flow model. This compensation is achieved by considering for each cell a flow in a third fictitious direction, y, resulting a three-dimensional space (x, y, z) that will correspond to the two-dimensional space (x, z). For the mathematical calculation convenience, the dimension of the cell in the fictitious direction is taken equal with 1:

$$\Delta y = 1 \tag{10}$$

By noting:

$$\Delta t \equiv v_s - v_n \tag{11}$$

eqn (9) becomes:

$$\rho \Delta z (u_e - u_w) + \rho \Delta x (w_h - w_l) = \rho \Delta x \Delta z \Delta v \tag{12}$$

For the cell denoted by indices (i, k), the above equation may be written as:

$$\rho \Delta z_k (u_{k,i-1} - u_{k,i}) + \rho \Delta x_i (w_{k-1,i} - w_{k,i}) = \rho \Delta x_i \Delta z_k \Delta v_{k,i} \tag{13}$$

where: $\rho \Delta x_i \Delta z_k \Delta v_{k,i}$ represents the mass algebraically added to cell (i, k) in order to correct the mass balance equation. Let us demonstrate that the algebraic sum of the mass added to each cell is null for overall system. That is:

$$\sum_{i=1}^l \sum_{k=1}^n \Delta x_i \Delta z_k \Delta v_{k,i} = \sum_{i=1}^l \sum_{k=1}^n [\Delta z_k (u_{k,i-1} - u_{k,i}) + \Delta x_i (w_{k-1,i} - w_{k,i})] = 0 \tag{14}$$

By convention, for the overall system, the flow which enters in through the boundaries is denoted by indices '0' and the flow which goes out through the boundaries is denoted by indices 'l' and 'n' for x- and z-directions, respectively (Fig. 4).

In steady state, the conservation of mass for the whole system states that the flow of mass which enters in and goes out through the whole system boundaries is balanced, that is:

$$\sum_{i=1}^l \Delta x_i (w_{0i} - w_{ni}) + \sum_{k=1}^n \Delta z_k (u_{k0} - u_{kl}) = 0 \tag{15}$$

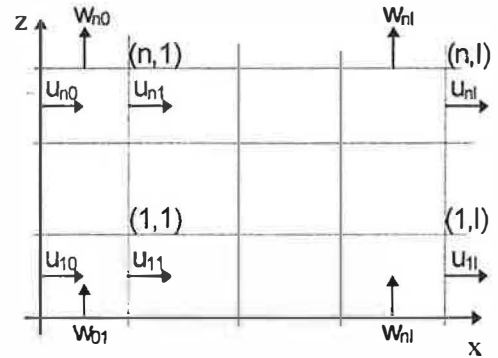


Fig. 4. Conventional notation of the velocity components in a two-dimensional grid.

The mass flow from one cell to another is added when the velocity is towards the cell and subtracted when the velocity is away from the cell. For internal boundaries of the cells, the total sum of the flow will be null, since the flow is added to a cell and subtracted from a neighbouring cell (Fig. 4). With eqn (15), eqn (14) becomes:

$$\begin{aligned} & \sum_{k=1}^n \left[\Delta z_k \left(\sum_{i=0}^{l-1} u_{ki} - \sum_{i=1}^l u_{ki} \right) \right] + \sum_{i=1}^l \left[\Delta x_i \left(\sum_{k=0}^{n-1} w_{ki} - \sum_{k=1}^n w_{ki} \right) \right] \\ &= \sum_{k=1}^n \left[\Delta z_k \left(u_{k0} + \sum_{i=0}^{l-1} u_{ki} - \sum_{i=0}^{l-1} u_{ki} - u_{kl} \right) \right] \\ &+ \sum_{i=1}^l \left[\Delta x_i \left(w_{0i} + \sum_{k=1}^{n-1} w_{ki} - \sum_{k=1}^{n-1} w_{ki} - w_{ni} \right) \right] = 0 \tag{16} \end{aligned}$$

The mass correction affects the other transport equations in which mass is involved.

2.4. Correction of energy balance equation

The correction introduced in the continuity equation will be reflected by a term in the energy equation. This correction term is related to the energy transported by the corrected mass. In the three-dimensional discrete space (x, y, z), the conservation of mass for a cell states that:

$$\text{div d(V)} \equiv \frac{u_e - u_w}{\Delta x} + \frac{v_n - v_s}{\Delta y} + \frac{w_h - w_l}{\Delta z} = 0 \tag{17}$$

Since the correction may be seen as a flow on only one surface in the fictitious direction, then:

$$v_s = 0 \Rightarrow v_s - v_n \equiv \Delta v = -v_n \tag{18}$$

and considering the temperature in the fictitious direction to have the same value as the one in the control volume, then the temperature on this surface is the temperature of the cell centre (point P in Fig. 2), and

$$\frac{(\rho v \theta)_n - (\rho v \theta)_s}{\Delta y} = \frac{(\rho v \theta)_n}{\Delta y} = \rho \theta \frac{v_n}{\Delta y} \tag{19}$$

From eqn (17) results:

$$\frac{u_e - u_w}{\Delta x} + \frac{w_h - w_l}{\Delta z} = -\frac{v_n - v_s}{\Delta y} = -\frac{v_n}{\Delta y} \quad (20)$$

therefore the equation of energy balance becomes:

$$\begin{aligned} \rho \frac{\partial \theta}{\partial t} = & -\rho \frac{(u\theta)_e - (u\theta)_w}{\Delta x} - \rho \frac{(w\theta)_h - (w\theta)_l}{\Delta z} \\ & + \frac{\left(\Gamma \frac{\partial \theta}{\partial x}\right)_e - \left(\Gamma \frac{\partial \theta}{\partial x}\right)_w}{\Delta x} + \frac{\left(\Gamma \frac{\partial \theta}{\partial z}\right)_h - \left(\Gamma \frac{\partial \theta}{\partial z}\right)_l}{\Delta z} \\ & + S_\theta + \rho \theta \left(\frac{u_e - u_w}{\Delta x} + \frac{w_h - w_l}{\Delta z}\right) \end{aligned} \quad (21)$$

Equation (21) describes the dynamic behaviour of temperature in a two-dimensional discrete-space (x, z) in which the (continuous) divergence of velocities is null.

Equation (21) may be considered a general representation. The numerical integration method for this differential equation with respect to time and differencing scheme for discretization in space becomes a free choice. The finite difference equations presented by Patankar [2] and considered by Awbi [4] are obtained as a particular solution of eqn (21) by applying the upwind difference scheme for space and Euler implicit method for time numerical integration.

3. Numerical simulation

The discretization of eqn (21) requires the application of a finite difference scheme. From the set of differencing schemes that may be used only the upwind scheme will be given as an example. Applying a finite differential scheme, eqn (21) becomes an ordinary differential equation with respect to time. Numerical integration of this equation by using Euler implicit method yields the same equation as the one presented by Patankar [2], Awbi [4] and used by commercial CFD programs.

In the upwind difference scheme (or donor cell method), the values of θ at the control surface (i.e. w, e, l and h surfaces) are taken as the value of upstream node point:

$$\theta_c = \theta \quad \text{for } u_c > 0 \quad \text{and} \quad \theta_c = \theta_E \quad \text{for } u_c < 0 \quad (22)$$

and similarly for θ_w , θ_l and θ_h . Using notation $[[A]]$ to denote the greater of A and 0, the first and the second term of eqn (21) may be written as:

$$\begin{aligned} & -\rho \left[\frac{(u\theta)_e - (u\theta)_w}{\Delta x} + \frac{(w\theta)_h - (w\theta)_l}{\Delta z} \right] \\ & = \left[\frac{1}{\Delta x} ([[u_w]] \theta_w - [[-u_w]] \theta - [[u_e]] \theta + [[-u_e]] \theta_E \right] \\ & + \rho \left[\frac{1}{\Delta z} ([[w_l]] \theta_L - [[-w_l]] \theta - [[w_h]] \theta + [[-w_h]] \theta_H \right] \end{aligned} \quad (23)$$

The third and the fourth right-hand terms of eqn (21) may be written as:

$$\begin{aligned} \frac{\left(\Gamma \frac{\partial \theta}{\partial x}\right)_e - \left(\Gamma \frac{\partial \theta}{\partial x}\right)_w}{\Delta x} & \cong \frac{1}{\Delta x} \left(\Gamma_e \frac{\theta_E - \theta}{\delta x_e} - \Gamma_w \frac{\theta - \theta_w}{\delta x_w} \right) \\ \frac{\left(\Gamma \frac{\partial \theta}{\partial z}\right)_h - \left(\Gamma \frac{\partial \theta}{\partial z}\right)_l}{\Delta z} & \cong \frac{1}{\Delta z} \left(\Gamma_h \frac{\theta_H - \theta}{\delta z_h} - \Gamma_l \frac{\theta - \theta_l}{\delta z_l} \right) \end{aligned} \quad (24)$$

With the notations:

$$\begin{aligned} a = & -\frac{[[-u_w]]}{\Delta x} - \frac{[[u_e]]}{\Delta x} - \frac{[[-w_l]]}{\Delta z} - \frac{[[w_h]]}{\Delta z} + \frac{u_e - u_w}{\Delta x} \\ & + \frac{w_h - w_l}{\Delta z} - \frac{1}{\rho \Delta x} \left(\frac{\Gamma_e}{\delta x_e} \right) - \frac{1}{\rho \Delta x} \left(\frac{\Gamma_w}{\delta x_w} \right) \\ & - \frac{1}{\rho \Delta z} \left(\frac{\Gamma_h}{\delta z_h} \right) - \frac{1}{\rho \Delta z} \left(\frac{\Gamma_l}{\delta z_l} \right) \end{aligned} \quad (25)$$

$$a_w = \frac{[[u_w]]}{\Delta x} + \frac{1}{\rho \Delta x} \frac{\Gamma_w}{(\delta x)_w} \quad (26)$$

$$a_E = \frac{[[-u_e]]}{\Delta x} + \frac{1}{\rho \Delta x} \frac{\Gamma_e}{(\delta x)_e} \quad (27)$$

$$a_L = \frac{[[w_l]]}{\Delta z} + \frac{1}{\rho \Delta z} \frac{\Gamma_l}{(\delta z)_l} \quad (28)$$

$$a_H = \frac{[[-w_h]]}{\Delta z} + \frac{1}{\rho \Delta z} \frac{\Gamma_h}{(\delta z)_h} \quad (29)$$

eqn (21) may be written:

$$\frac{d}{dt} \theta = a\theta + a_w \theta_w + a_E \theta_E + a_L \theta_L + a_H \theta_H \quad (30)$$

or, if there are internal sources, S , eqn (21) becomes:

$$\frac{d}{dt} \theta = a\theta + a_w \theta_w + a_E \theta_E + a_L \theta_L + a_H \theta_H + \frac{S}{\rho} \quad (31)$$

It is easy to observe that:

$$a = a_w + a_e + a_L + a_H \quad (32)$$

or the rule of coefficients mentioned by Patankar [2] is respected.

If the Euler implicit method is used to integrate numerically eqn (31), then:

$$\frac{\theta - \theta^o}{\Delta t} \cong \frac{d}{dt} \theta = a\theta + a_w\theta_w + a_e\theta_e + a_L\theta_L + a_H\theta_H + \frac{S}{\rho} \quad (33)$$

where $\theta \equiv \theta(t)$ and $\theta^o \equiv \theta(t - \Delta t)$. Then eqn (33) may be written as:

$$\left(\frac{1}{\Delta t} - a\right)\theta = a_w\theta_w + a_e\theta_e + a_L\theta_L + a_H\theta_H + \frac{S}{\rho} + \frac{\theta^o}{\Delta t} \quad (34)$$

Writing the source term as $S = S_C + S_p\theta$ and multiplying eqn (34) by $\rho\Delta x\Delta y$ it becomes exactly the same as the final finite difference equation presented by Patankar [2] and widely used in CFD programs:

$$a'\theta = a'_w\theta_w + a'_e\theta_e + a'_L\theta_L + a'_H\theta_H + b' \quad (35)$$

with:

$$\begin{aligned} a'_w &= \rho \Delta x \Delta z a_w; & a'_e &= \rho \Delta x \Delta z a_e; \\ a'_L &= \rho \Delta x \Delta z a_L; & a'_H &= \rho \Delta x \Delta z a_H; \end{aligned} \quad (36)$$

$$b' = S_C \Delta x \Delta z + a'^o \theta^o; \quad \text{with } a'^o = \frac{\rho^o \Delta x \Delta z}{\Delta t} \quad (37)$$

$$a' = a'_w + a'_e + a'_L + a'_H + a'^o - S_p \Delta x \Delta z \quad (38)$$

The energy eqn (31) is implemented in MATLAB, having the flow field given as computed by CFD software PHOENICS. As the numerical integration method is a free choice, any method available in MATLAB can be used. The details regarding the implementation are given by Ghiaus et al. [7]. Figure 5 presents a sequence of temperature distribution as obtained by the model. The number of nodes for the numerical grid generation is 24 (in x -axis) by 24 (in y -axis). The velocity field is fixed during the simulation of temperature distribution. The implementation is achieved in MATLAB and can be run on the same platforms as MATLAB (Windows or Unix). On a Windows platform (Pentium 133 MHz) the numerical simulation time is approximately 5 s for a process that lasts in reality 60 s.

4. Experimental facility and results

In order to validate the mathematical model, experiments were performed in a test-cell, located at Delft University of Technology, 52°N and 4°6'E. The cell room has internal dimensions of 3.2 × 3.9 × 2.68 (m) and exter-

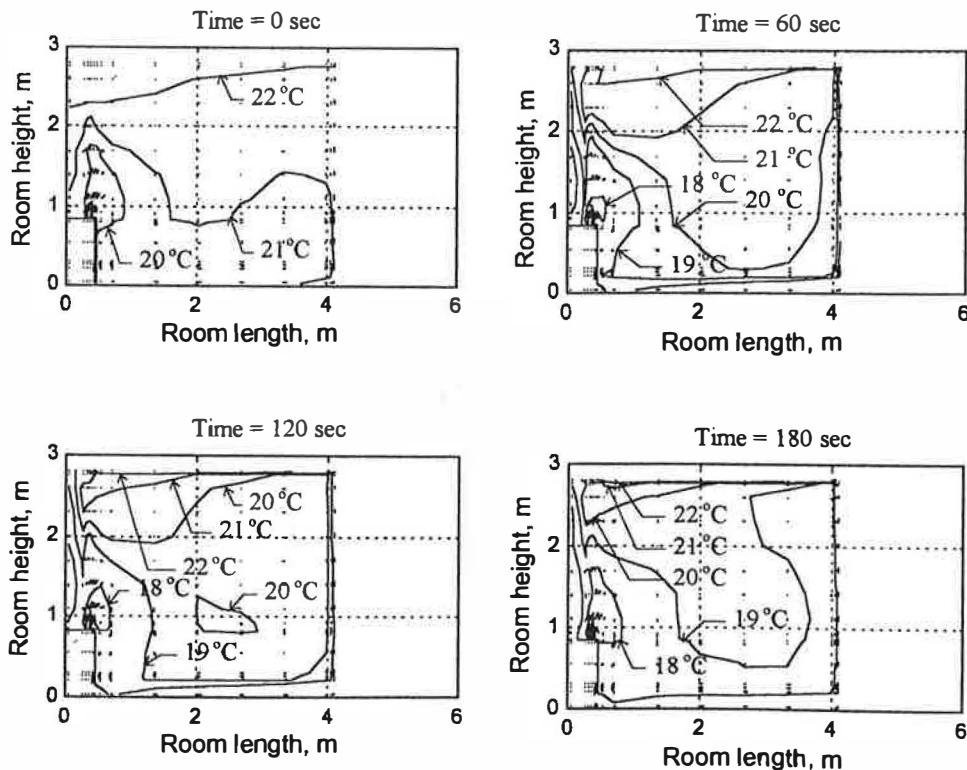


Fig. 5. Room temperature distribution numerically simulated with a sample time-step of 60 s.

Table 2
Specifications of the materials used for the roof, walls and floor

Layer type	Thickness [mm]	Conductivity [$\text{W m}^{-1} \text{K}^{-1}$]	Density [kg m^{-3}]	Heat capacity [$\text{J kg}^{-1} \text{K}^{-1}$]
Roof and walls:				
Steel	0.6	52	7800	500
Polystyrene	148	0.034	20	1300
Floor:				
Carpet	5	0.06	160	2500
Aluminium	2.5	200	2800	880
Plywood	18	0.17	700	1880
Polystyrene	150	0.034	20	1300

nal ones of $3.4 \times 4.2 \times 3.0$ (m). The room window ($3.1 \times 1.9 \text{ m}^2$), with the glazing global heat transfer coefficient of $2.7 \text{ W m}^{-2} \text{ K}^{-1}$, has the azimuth 30°E . The roof and the walls are constructed from light-weight sandwich plates, (polystyrene with steel plate layers on both sides) having the heat transfer coefficient equal to $2.7 \text{ W m}^{-2} \text{ K}^{-1}$ and the floor is made of polystyrene, plywood, aluminium and carpet on top. The global heat transfer coefficient of the floor is $1.9 \text{ W m}^{-2} \text{ K}^{-1}$. The specifications of the above materials are given in Table 2. The temperature was measured at points on a nine-node grid, symmetrically distributed in a perpendicular plane on the window surface. A fan-coil, installed under the window introduces, by means of two separate coils, cool or warm air for cooling or heating, respectively. The operation characteristics of the fan-coil are given in Table 3. The simulation results were compared with the experimental ones, both in time and in frequency domain. A comparison of a step response at the start-up (in the morning) is shown in Fig. 6. The model gives a good response at the beginning, but, because the simulated wall temperature was assumed to be constant, in the last part of the response the influence of the actual variable wall temperature can be observed. However, from the point of view of controlling the temperature it is more important to consider a frequency response comparison. Using the tools of control theory, the frequency response (Bode diagrams) can be easily achieved. To obtain the frequency response, the inlet air temperature was varied

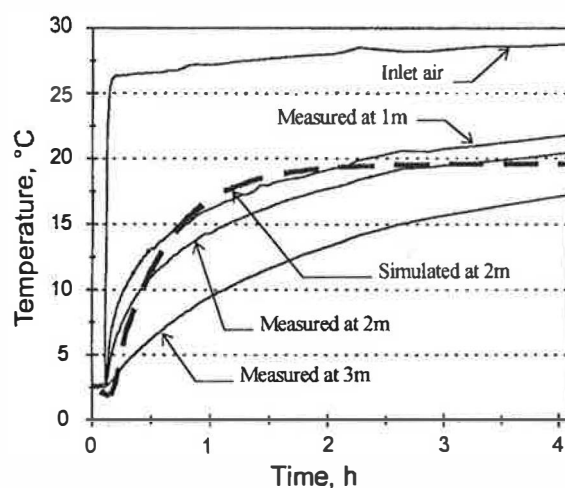


Fig. 6. Mean temperature step response simulated and measured in several horizontal planes.

according to a function obtained as a sum of sine waves of different frequency, which are typical for normal operation of a fan-coil. The comparison for a point in the occupied zone is given in Fig. 7. The response was achieved by varying the inlet temperature of the air so that the frequencies contained in the signal covered the domain of interest for control purposes.

5. Conclusions

The discretization of the continuity equation introduces an error due to non-linear velocity field. The method presented corrects the continuity and energy equations for discrete space models. The correction term may be seen either as a flow in a fictitious direction or as a source of mass, so that:

- If the correction term is positive, it means that there was a removal of mass from the elementary cell and some mass should be added to compensate.

Table 3
Operation characteristics of the fan-coil

Fan-coil characteristics	Low speed	Medium speed	High speed
Air volume flow rate [$\text{m}^3 \text{h}^{-1}$]	225	330	600
Heating power at $90/70 \text{ C}$ [kW]	2	3	4
Cooling power at $6/12 \text{ C}$ [kW]	1	1.2	2

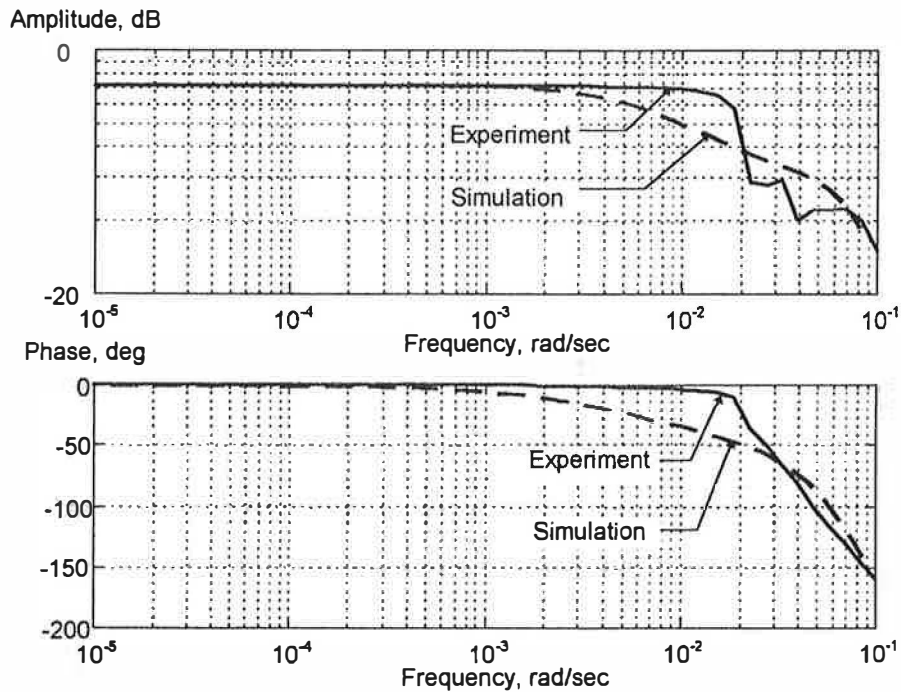


Fig. 7. Comparison between simulation and experimental results in frequency domain for a point in the occupied zone.

- If the correction term is negative, it means that there was an addition of mass to the elementary cell and some mass should be removed to compensate.

A remark should be made: accepting that the stationary velocity field is correct, that is the divergence of velocities is null, it is possible that the conservation of mass will not be respected for some elementary cells of the discrete space system. However, since the model is in discrete space form, the conservation of mass should be respected for each elementary cell. The mass conservation law in steady state for constant density, continuous space systems is:

$$\frac{\partial}{\partial x} u + \frac{\partial}{\partial y} v + \frac{\partial}{\partial z} w = 0 \quad (39)$$

and for constant density, discrete space systems is:

$$\frac{u_z - u_w}{\Delta x} + \frac{v_n - v_s}{\Delta y} + \frac{w_h - w_l}{\Delta z} = 0 \quad (40)$$

Accepting eqn (39) to be true means that eqn (40) does not necessarily stand for each cell. In fact, eqn (39) should be satisfied for continuous systems. Reciprocally, accepting eqn (40) to be true means that eqn (39) does not necessarily stand for each point in the continuous system. However, eqn (40) should be satisfied in a discrete space system. However, the mass conservation law should be respected in the system, whether it is described in continuous or discrete form. In fact, accepting that the velocity field is correct, then eqn (39) stands and a correction

is introduced to have the mass conservation respected also in each elementary cell. Since the conservation of mass should be respected also in the system as a whole, if the velocity field is correct, the total algebraic sum of mass exchanged in the fictitious direction should equal zero.

The corrected dynamic model of temperature may be integrated using any numerical integration method (e.g. Euler implicit or explicit, Runge–Kutta, Adams or Gear). As these integration methods use variable time steps, the time efficiency of these methods is very good. In literature, the energy differential equation is discretized using implicit method. When the flow field is changed, a set of algebraic equations is to be solved in one step (by inverting the matrix of coefficients) or by iteration (an initial guess followed by an iterative calculation). The inverse of the matrix and the iterative procedure are far more time consuming than integrating with an explicit method with variable time step (for a standard size room about 10^3 – 10^5 times faster).

Acknowledgements

The experimental measurements were carried out at Laboratory of Refrigerating Engineering and Indoor Climate Technology, Delft University of Technology, The Netherlands, X. Peng and A.H.C. van Paassen, from the same laboratory, provided the flow field calculations.

References

- [1] Fanger PO. Thermal comfort. Malabar (Florida): Robert E. Krieger Publishing Company, 1982.
- [2] Patankar V. Numerical heat transfer and fluid flow. New York: McGraw-Hill Inc., 1980.
- [3] Chen Q. Indoor airflow, air quality and energy consumption of buildings. Ph.D. thesis, Delft University of Technology, Delft, 1988.
- [4] Awbi HB. Ventilation of buildings. E and FN Spon, 1991.
- [5] Peng X, van Paassen AHC, Chen Q. A type of calculation of indoor dynamic temperature distribution. Proceedings of System Simulation of Buildings Conference. Liege, 1994.
- [6] Ghiaus C. Numerie and expert control of air conditioning installations. Ph.D. thesis. Technical University of Civil Engineering, Bucharest, 1996.
- [7] Ghiaus C, Peng X, van Paassen AHC. A state-space representation of the dynamic model of air temperature distribution. Proceedings of 19th International Congress of Refrigeration. The Hague, 1995.